Journal of Visualization, Vol. 2, No. 2 (1999) 185-194

Numerical Visualization of Vortical Structures in a Spatially Evolving Turbulent Compressible Mixing Layer

Liou, T-M.* and Hwang, P-W.*

* Department of Power Mechanical Engineering, National Tsing Hua University, Hsinchu, Taiwan 30043, R.O.C.

Received 25 November 1998.
Revised 27 April 1999.

***Abstract*:** Large-eddy simulations are performed to numerically visualize the generation of streamwise vortical structures and its interaction with spanwisely rolled-up coherent vortical structure during the spatial development of a turbulent supersonic/subsonic mixing layer at convective Mach number M_c=0.51. Time-dependent three-dimensional compressible conservation equations were solved with a subgrid-scale turbulence model. The numerical code used the finite-volume technique, which adopted alternately in temporal discretization the second-order, explicit MacCormack's and modified Godunov's schemes. Both transverse and spanwise perturbations were imposed initially for promoting the formation of spanwise rollers and counter-rotating streamwise vortices, respectively. Numerical visualizations are presented in terms of time-sequence isopressure surfaces and vorticity contours of spanwise and streamwise components. The results show that the spatial growth of three-dimensional vortical structures, in particular, the formation of chain-link-fence type structures, is adequately captured by the present computations. Vorticity dynamics is further analyzed, for the first time, to identify the dominant roles played by the convection effect followed by the vortex stretching effect on affecting the evolution of streamwise and spanwise vortical structures, respectively, for M_c<0.6.

***Keywords*:** compressible, spatially evolving, mixing layer, perturbation, streamwise vortex

1. Introduction

Turbulent free-shear flows are encountered in many engineering applications and have been one of the most active areas of research in fluid mechanics. They are often selected to preliminarily verify the predictability of turbulence models since the pressure gradient and viscous diffusion are negligible without wall confinements. However, the validations are mostly limited to mean flow fields. The present study focuses on the spatially developing free shear layer generated by turbulent mixing of two coflowing fluid streams, as shown schematically in Fig. 1.

The large quasi-two-dimensional (2-D) coherent vortical structures in subsonic turbulent free shear flows were first observed by experimental investigations (Brown and Roshko, 1974; Winant and Browand, 1974) which drastically altered researchers' perceptions of the mixing process in these flows. Subsequent experimental studies (Breidenthal, 1981; Jimenez, 1983; Bernal and Roshko, 1986; Lasheras et al., 1986) further revealed the large-scale spanwise variation of these quasi-2-D coherent vortical structures due to the presence of a streamwise vorticity component. Moreover, increased research effort has been directed toward the compressible turbulent mixing layer due to mixing and combustion issues related to supersonic flight (Lele, 1994). Thus, three-dimensional (3-D) experimental measurements and theoretical predictions on the compressible mixing layer problem are very desirable for a better understanding of the relevant physics.

Three-dimensional compressible mixing layer simulations have been performed by Soetrisno et al. (1989), Sandham and Reynolds (1991), Leep et al. (1993), and Ragad et al. (1994) using a temporally evolving approach and by Grinstein et al. (1988) and Gathmann et al. (1993) using a spatially evolving approach. The main difference

between the results of the two approaches is that the temporally evolving calculations essentially describe the time evolution of the flow in compact regions, although practical flows evolve both in space and time, and can not thus capture the behaviors such as asymmetric entrainment and any effects resulting from the stream selection rule of Dimotakis (1991). As for the spatially evolving approach, Grinstein et al. (1988) investigated subsonic/subsonic shear layers using a compressible flow solver with a flux-corrected transport algorithm whereas Gathmann et al. (1993) studied confined supersonic/supersonic shear layers using a compressible flow solver with a piecewise parabolic method. In contrast, limited attention has been drawn to examine supersonic/subsonic shear layers which are often encountered in the practical ramjet combustor and ejector and are associated with the noise problem caused by a supersonic jet discharging into a subsonic stream.

Jimenez (1983) experimentally found that the locations of streamwise vortices are often dependent on perturbations that originate from wind-tunnel screens or nicks in the nozzle lip. The experiment of Lasheras et al. (1986) also indicated that the position where the formation of 3-D structures as first observed varies substantially with the location and the intensity of the upstream disturbances. Nygaard and Glezer (1991) experimentally visualized the effects of spanwise-nonuniform excitation on a plane mixing layer. They found that under appropriate forcing the flow pattern evolves into a series of diamond-shaped cells arranged in a chain-link-fence pattern. These experimental observations suggest the important role played by the initial disturbances in affecting the location of the transition to three-dimensionality in the plane mixing layer. It is based on the above fact that small-amplitude 3-D perturbations were introduced into an otherwise 2-D flowfield to trigger the 3-D instabilities in the aforementioned 3-D compressible mixing layer simulations (Grinstein et al., 1988; Soetrisno et al., 1989; Sandham and Reynolds, 1991; Gathmann et al., 1993; Leep et al., 1993; Ragad et al., 1994).

Since the spatial evolutionary structures observed in the incompressible mixing layer experiment of Nygaard and Glezer (1990) have not been reported in the experiments of the compressible mixing layer which only presented mean and fluctuating velocity component profiles, the objectives of the present work are to perform a detailed investigation of the onset of 3-D instabilities in a spatially evolving planar supersonic/subsonic shear flow at convective Mach number M_c=0.51 and to find whether the spatial evolutionary structures observed by Nygaard and Glezer (1990) can be qualitatively reproduced in the compressible mixing layer for M_c<0.6. Emphasis is on numerical visualization of the formation and development of streamwise vortices in the mixing layer and their interaction with the spanwise vortex roll-ups under a given set of 3-D perturbations at upstream inlet stage (x=0). The limitation of the present study to M_c<0.6 is based on a review of the existing data. Sandham and Reynolds (1991), Leep et al. (1993), and Ragad et al. (1994) found that the temporally evolved oblique waves have a constant angle $\theta \approx 45°$ with the spanwise direction for M_c<0.6 and obey the correlation $M_c \cos\theta \approx 0.6$ for M_c>0.6. It is thus expected that the chain-link-fence pattern may prevail from the incompressible mixing layer regime to the compressible mixing layer regime as long as M_c<0.6.

2. Numerical Method

A detailed description of the governing equations and subgrid-scale model adopted in the present large-eddy simulations, numerical algorithm, and boundary conditions is available in Liou et al. (1995, 1999). The initial conditions are based on the expreiments (Samimy and xlliott, 1990) with follwing flow parameters: velocity (u_1=492 m/s, u_2/u_1=0.36), density (q_1=1.024 kg/m^3, q_2/q_1=0.64), convective Mach number (M_c=0.51), and Reynolds number (Re_θ=21500).

As pointed out in Introduction, to predict the formation of streamwise vortices in a plane mixing layer 3-D perturbations need to be incorporated into the original 2-D perturbations which trigger the formation of spanwise vortices (Liou et al., 1995). The 3-D instabilities were triggered through a spanwisely spatial sinusoidal perturbations of the cross-stream velocity fields as originally suggested by Grinstein et al.(1988) and modified in the present study at $t^*=t/(L/u_\alpha)\geq 7$ (time attaining 2-D development) where t is time, L=60 cm the longitudinal length of computational domain, and $u_a=0.5(u_1+u_2)$ the average inlet velocity. The rms spanwise perthurbation level was set up at 5% of the average inlet velocity u_a and only two wavelengths (λ_z=15 cm) were included in the spanwise extent to simulate a selected case reported in published experimental work (Nygaard and Glezer, 1990).

3. Results and Discussion

The validation of the present numerical simulation has been performed in terms of both mean and fluctuating velocity components available from the study of Samimy and Elliott (1990). Significant improvement has been attained (not shown here due to space limitation) in comparison with our previous 2-D simulation (Liou et al., 1995).

3.1 Three-dimensional Flow Visualization by Iso-surfaces

The numerical flow visualizations are shown in Fig. 1 in terms of iso-surfaces of spanwise ($\tilde{\omega}_z$=0.18$|\tilde{\omega}_z|_{max}$, z<0 in Figs. 1(a)-(b), color: silver) and streamwise ($|\tilde{\omega}_x|$=0.19$|\tilde{\omega}_x|_{max}$, z>0 in Figs. 1(a)-(b), color: green (positive) and

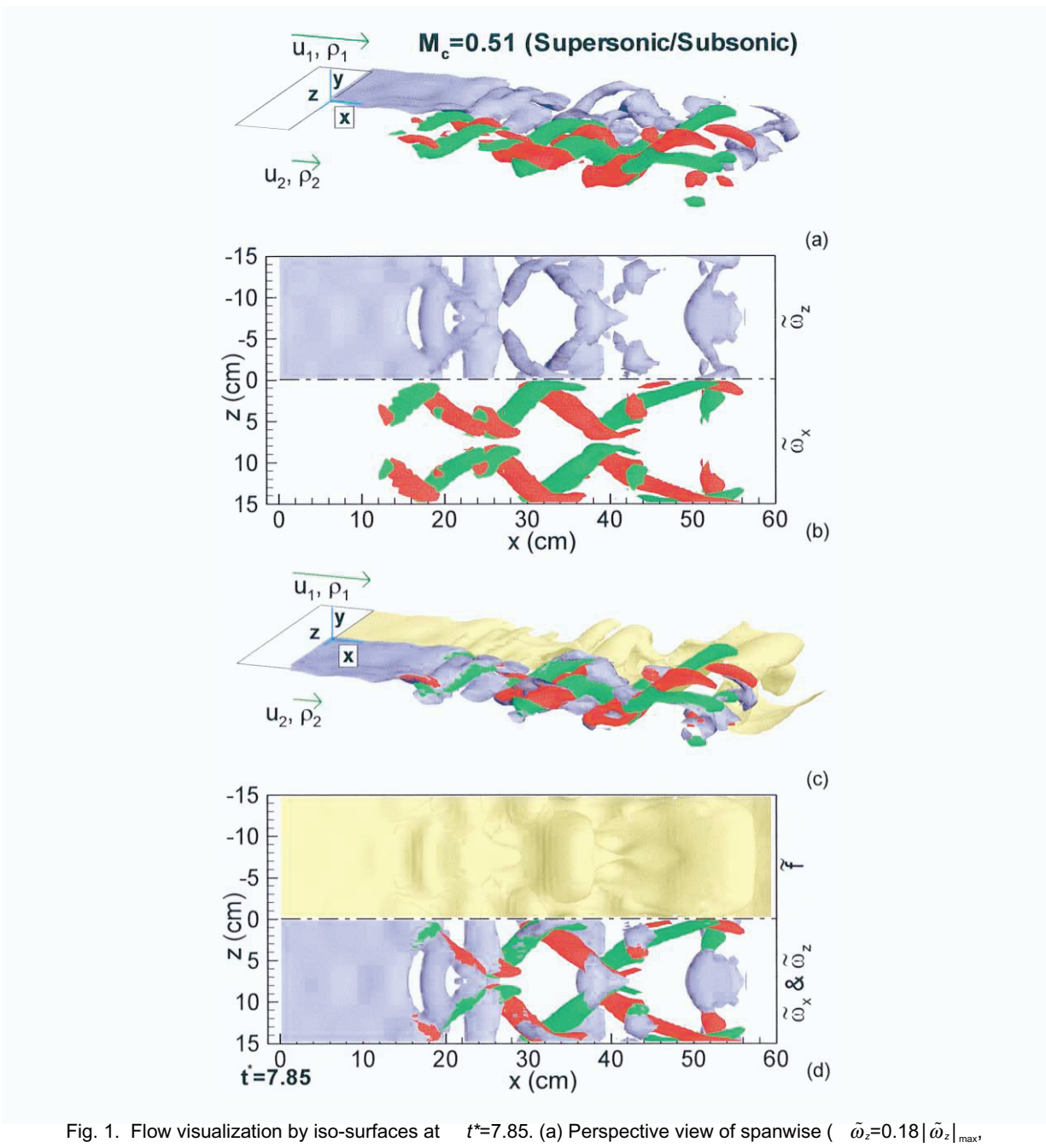

Fig. 1. Flow visualization by iso-surfaces at t^*=7.85. (a) Perspective view of spanwise ($\tilde{\omega}_z$=0.18$|\tilde{\omega}_z|_{max}$, z<0) and streamwise vorticities ($|\tilde{\omega}_x|$=0.19$|\tilde{\omega}_x|_{max}$, z>0, red: negative; green: positive); (b) Plan view of (a); (c) Perspective view of mixture fraction ($\tilde{f}$=0.5, z<0) and combination of spanwise and streamwise vorticities (z>0); (d) Plane view of (c).

red (negative)) vortices, mixture fraction ($\tilde{f}$=0.5, z<0 in Figs. 1(c)-(d), color: gold), and resultant vortices of streamwise and spanwise components (z>0 in Figs. 1(c)-(d)) at t*=7.85. Note that higher values of vorticities, $\tilde{\omega}_z$>0.18$|\tilde{\omega}_z|_{\max}$ and $|\tilde{\omega}_x|$>0.19$|\tilde{\omega}_x|_{\max}$, occur within the volumes enclosed by the surfaces depicted in Fig. 1. It is seen that the nominally 2-D spanwise roller ($\tilde{\omega}_z$ and $\tilde{f}$) prevail in the region of 0< x<15 cm are distorted in the spanwise direction by the appearance of streamwise vortices. The degree of distortion increases with increasing x and the vorticity and mixture fraction structures become highly 3-D and oblique. In particular, the streamwise vorticity components are shaped into diamond-shaped cells in a chain-link-fence pattern. The fence consists of alternative positive and negative $\tilde{\omega}_x$. It should be mentioned that the diamond-shaped structure presented in Fig. 1 is very similar to that observed experimentally by Nygaard and Glezer (1990, see Fig. 3(f) and Fig. 5 in their paper). The interaction of the streamwise vortices with the spanwise rollers can be observed with some detail in Figs. 1. (c)-(d) (z<0) which give a visualization of the formation of streamwise vortices superimposed on the spanwise vortices in terms of the equivortical iso-surfaces of $\tilde{\omega}_x$ and $\tilde{\omega}_z$. As one can see that the streamwise vortices, appearing in counter-rotating pairs and occurring in the region of the braids in response to sinusoidal coherent spanwise perturbations, are considered to be characteristic of three-dimensional mixing layers (Bernal and Roshko, 1986). The equi- $\tilde{f}$ iso-surfaces depicted in Figs. 1(c)-(d) (z<0) further revealed that the main effect of these large-scale coherent structures is to wrinkle and increase the interfacial area and, in turn, the mixing between the coflowing streams. From these observations, it appears that controlled spanwise perturbation can be an important mechanism for mixing control.

3.2 Evolution of the Instantaneous Iso-surfaces

The formation of the streamwise vortices and the interactions between streamwise and spanwise vortices can be further revealed by the temporal development of the isopressure surfaces in terms of plan view and instantaneous spanwise vorticity contours in z/λ_z=0 plane, as shown in Fig. 2. Visualizations of the pressure field are helpful since low-pressure regions are associated with strong rotation which, in turn, identify the areas where the most mixing occurs. The pressure of the surface plotted is approximately 80% above the pressure minimum and lower pressure values occur within the volumes enclosed by the surfaces.

Because the 3-D perturbation is introduced into the fluid flow at t*=7, the flowfield remains 2-D until t*=7.05 (Fig. 2(a)). As time elapses, the effect of 3-D perturbation propagates downstream gradually such that the upstream line vortex becomes zigzagging vortex (Fig. 2(b)). The upstream consecutive vortex cores in Figs. 2(b)-(j) are in the process of pairing, in a 3-D (helical) fashion with the vortices winding up around each other at the tips of the zigzags. As a result, a quasispanwise double helix vortex structure, as observed experimentally by Chandrsuda et al. (1978), is formed. The strain field between the rollers stretches the spanwise vorticity component leading to the generation of primary streamwise vortices (Fig. 2(d), x≈14 cm). The primary streamwise vortices bend in the spanwise direction and in turn create secondary streamwise vortices in place of the original spanwise vortices (Fig. 2(e), x≈22 cm). This evolution is repeated with increasing time and eventually the flow structures are arranged in diamond-shaped cells in a chain-link-fence pattern (Figs. 2(i)-(l)), as observed in the experiment of Nygaard and Glezer (1990). It is worth pointing out that the resulting flow structures are further characterized by having wavelengths longer in spanwise direction and shorter in streamwise direction, a phenomenon consistent with that observed in the work of Nygaard and Glezer (1990).

A closer examining of the primary and secondary streamwise vortices in the region of 14<x<26 cm depicted in Fig. 2(g) in terms of isopressure surfaces, one finds that vortical structures become clearer with increasing t* (Figs. 2(g)-(i)) and their legs tend to stretch out and touch on the downstream vortical structures. From a comparison of the upper and lower figures in each set of Figs. 2(h)-(i), it is clear that the aforementioned contact regions (lower figure) are the high strain-rate braid regions (upper figure) as evidenced by the red-color regions in the spanwise vorticity contours. The comparison also shows that at the contact regions the spanwise vortical structures actually consist of upper and lower vortices separated by the high strain-rate regions (Fig. 2(d), x≈14 cm; Fig. 2(e), x≈21 cm; Fig. 2(f); x≈12 cm and x≈28 cm; Fig. 2(g), x≈19 cm and x≈34 cm; Fig. 2(h), x≈11 cm and x≈26 cm; Fig. 2(i), x≈18 cm and x≈32 cm) which seem to retard the vortex pairing as the flow proceeds downstream. Comparing Fig. 2(i) with Fig. 1, one also finds that the isopressure surfaces can reveal the vortical flow structures. As t*>7.85, the well-organized vortical structures gradually break-down between the heads and legs (Fig. 2(j), x≈36 cm; Fig. 2(k), x≈42 cm; Fig. 2(l), x≈48 cm), a phenomenon also found in the simulations of temporally developing mixing layer by Ragad et al. (1994). Another observation is that the center of the shear layer gradually shifts towards the lower (slower stream) side as the flow proceeds downstream, which is an evidence of the inherently asymmetric entrainment in the planar shear flow (Koochesfahani et al., 1985). In summary, the

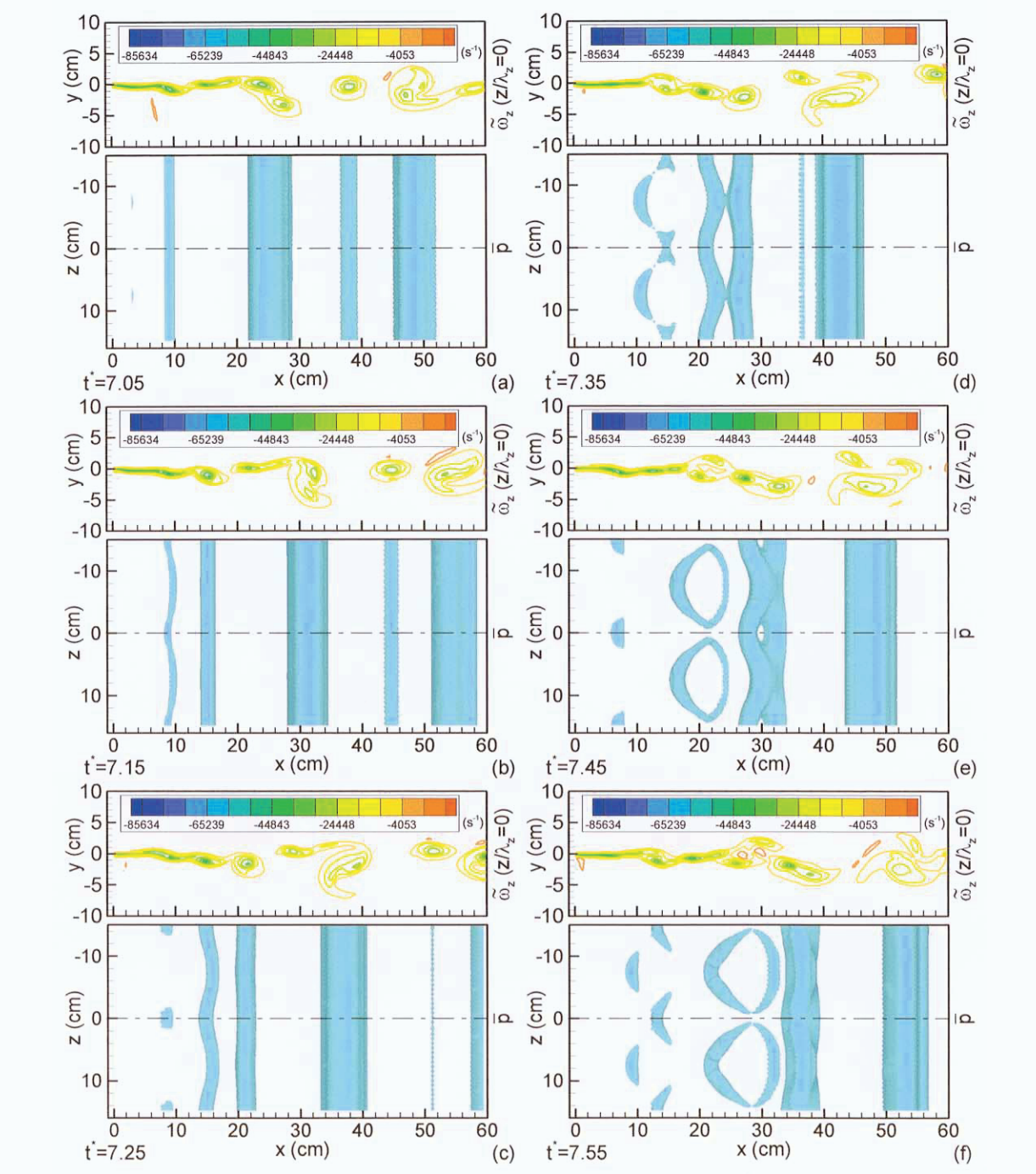

Fig. 2. For legend see next page.

isopressure surfaces plotted in Fig. 2 clearly demonstrates the undulating distortion of the spanwise rolls induced by the streamwise vortices and the stretching of the vortex rolls with their mergings with the streamwise vortices.

3.3 Vorticity Dynamics

To understand the physics underlying the spatially evolving turbulent mixing layer, it is useful to analyze the mechanisms of vorticity dynamics; nevertheless, this type of analysis has seldom been performed in the past. The vorticity equation for an inviscid, 3-D compressible flow can be expressed as

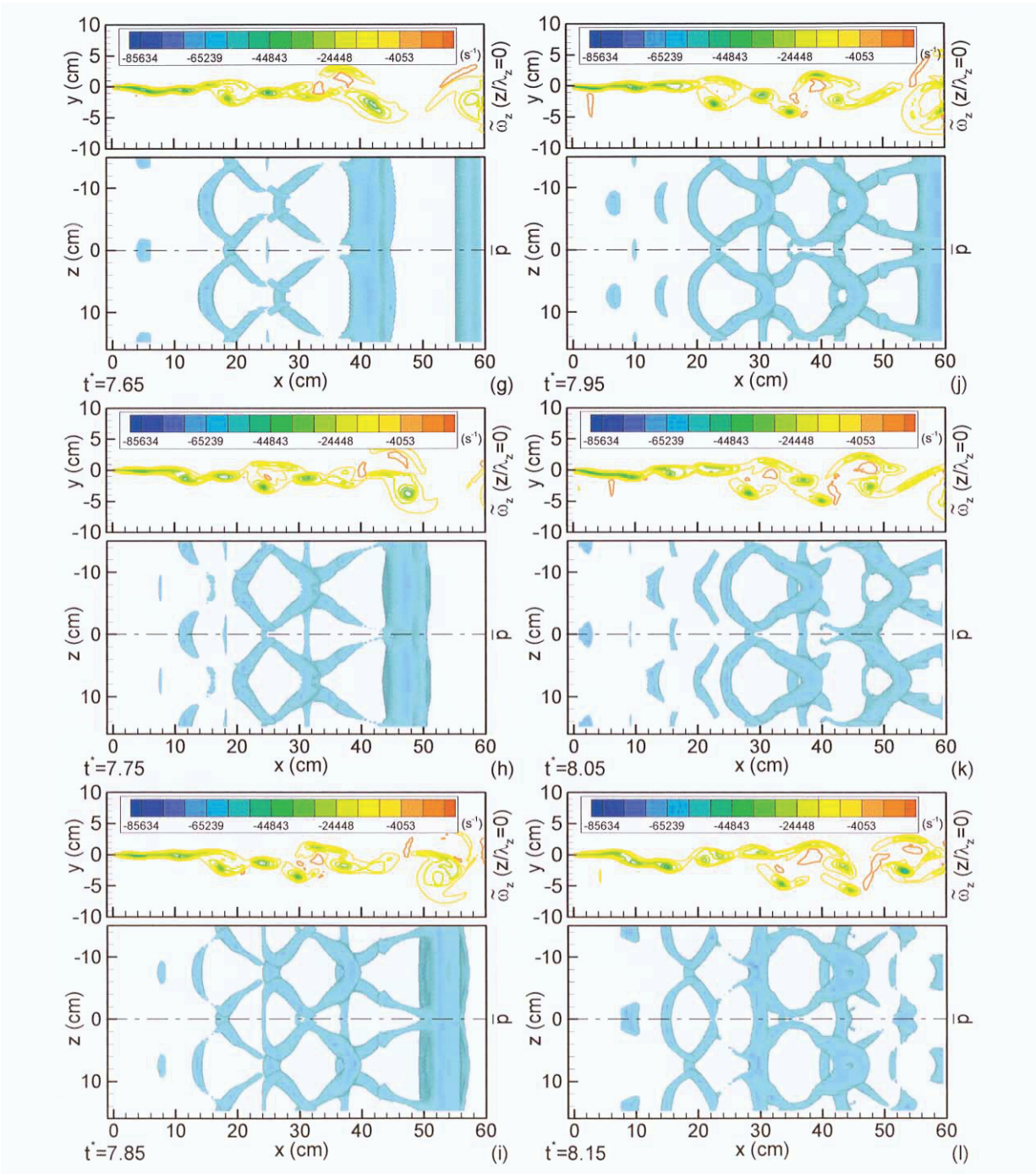

Fig. 2. Time sequence of plane view of isopressure surfaces ($\bar{p}=1.8\bar{p}_{min}$) and cross-cut side view of spanwise vorticity contours through the dash-dot line. From (a) to (l), t^*=7.05–8.15, Δt^*=0.1.

$$\frac{\partial\tilde{\omega}}{\partial t} = -(\tilde{\boldsymbol{V}}\cdot\nabla)\tilde{\omega} - \tilde{\omega}\ (\nabla\cdot\tilde{\boldsymbol{V}}) + (\nabla\bar{\rho}\times\nabla\bar{p})/\bar{\rho}^2 + (\tilde{\omega}\cdot\nabla)\,\tilde{\boldsymbol{V}} \tag{1}$$

That is, the rate of change of vorticity is due to four effects (convection, dilatation, baroclinic torque, and vortex stretching) corresponding to the terms on the right-hand side of Eq. (1). The instantaneous spanwise-averaged $\tilde{\omega}_x$ and $\tilde{\omega}_z$ contours and evolution of y-z plane-averaged magnitudes of these terms (Fig. 3(a)) in the x-component and z-component vorticity dynamics equations along the streamwise distance are depicted in Fig. 3 and Fig. 4, respectively. When t^* is increased, it is seen from $\tilde{\omega}_x$ contours in Fig. 3 that the extent of streamwise vorticity and $\partial\tilde{\omega}_x/\partial t$ correlates with the occurrence of 3-D flow structure, as evidenced by comparing Figs. 3(a)-(c) with Figs.

2(d), 2(f), and 2(i). Comparing Fig. 3 with Fig. 4, one finds that among the four terms on the right-hand side of Eq. (1), the convection term is the dominant one followed by the vortex stretching term in contributing to the time variation of $\tilde{\omega}_x$ or $\tilde{\omega}_z$. The effects of the dilatation and baroclinic terms are relatively small at M_c=0.51 investigated. One can also find that the structures of the longitudinal vortices are getting more intact as t^* is increased. The trend is reversed for the case of spanwise vortices.

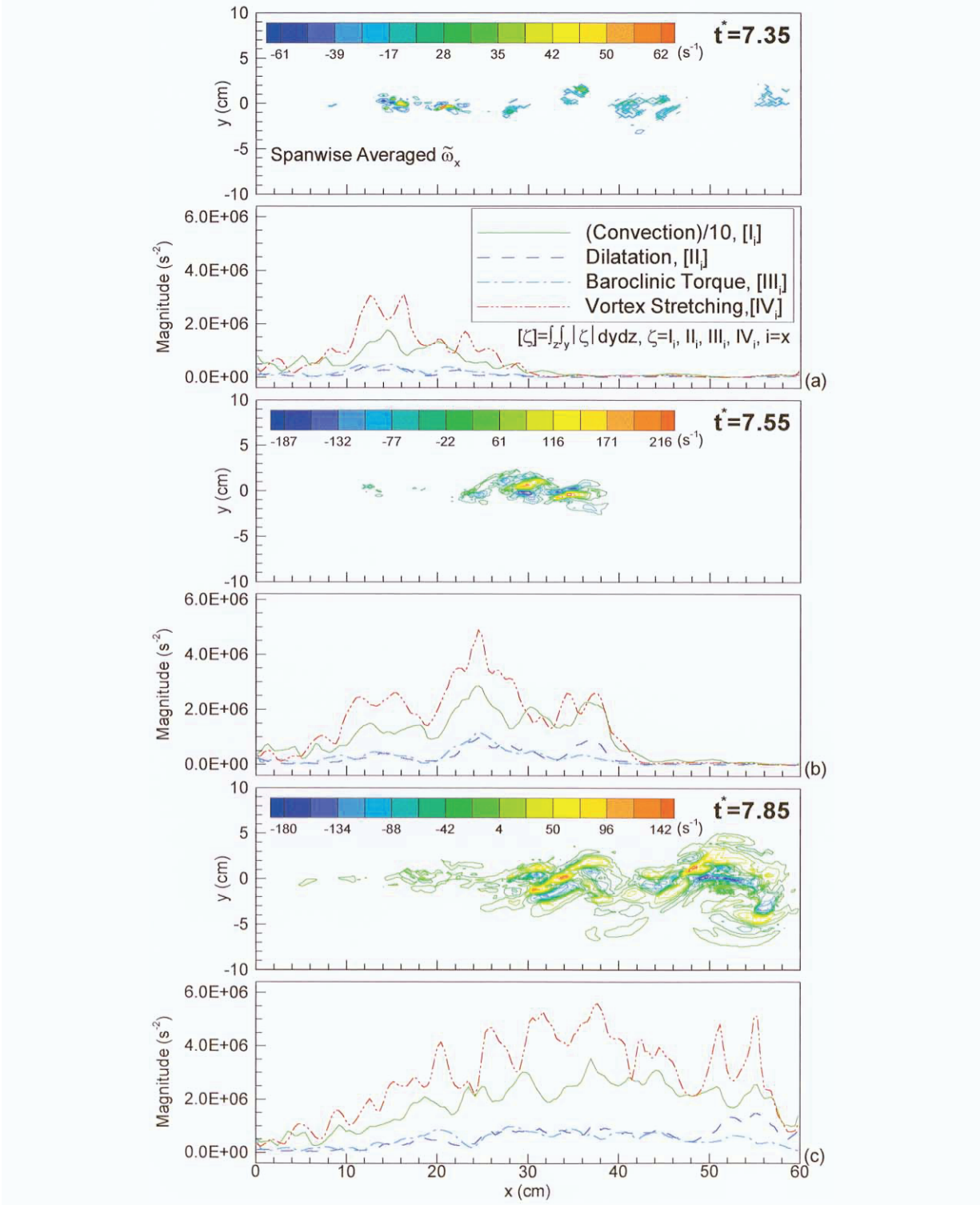

Fig. 3. Instantaneous spanwise-averaged $\tilde{\omega}_x$ contours and axial variation of y-z plane averaged contributions (i.e., the four terms on the right-hand side of Eq. (1)) to $\partial\tilde{\omega}_x/\partial t$. (a) t^*=7.35; (b) t^*=7.55; (c) t^*=7.85.

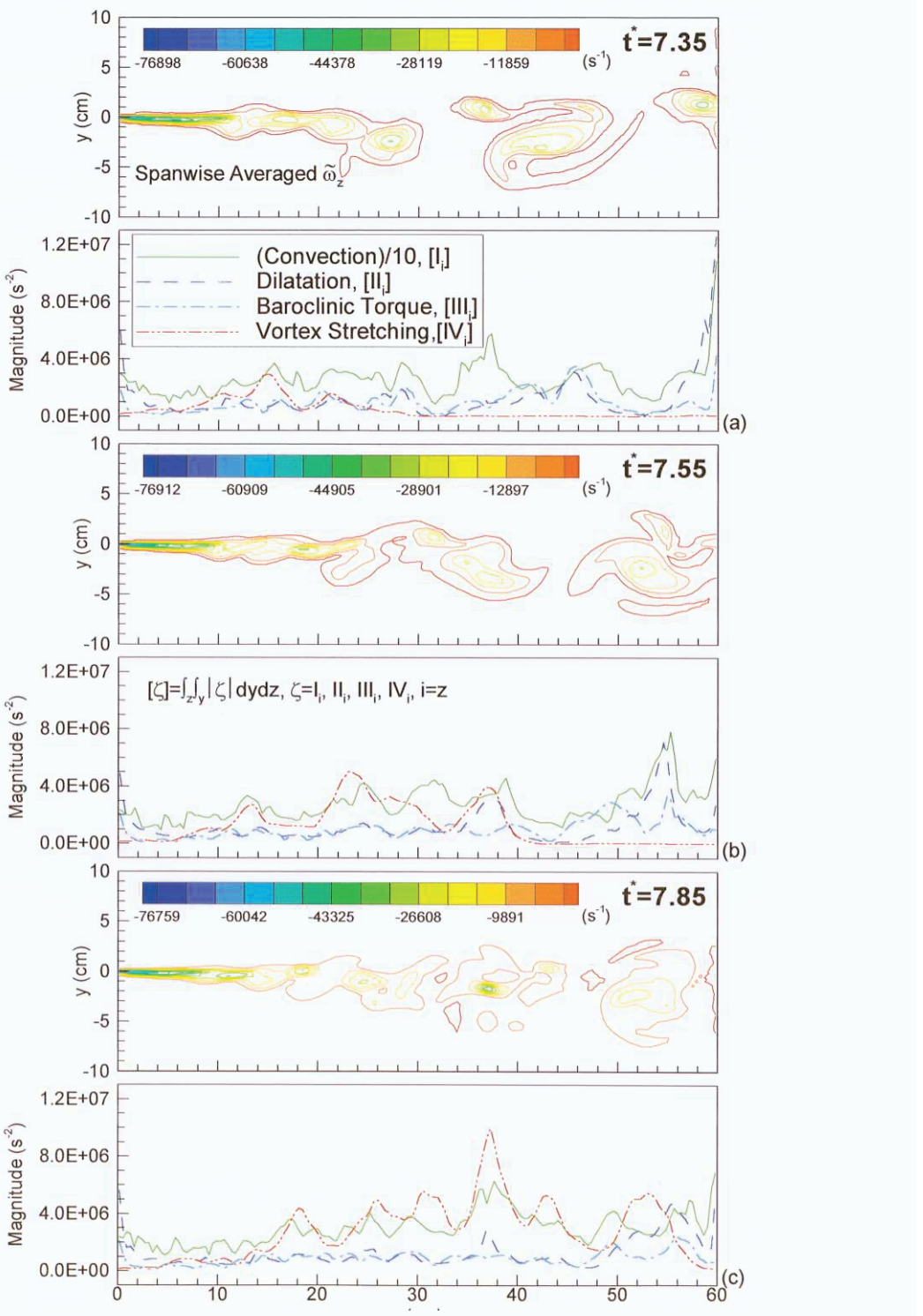

Fig. 4. Instantaneous spanwise-averaged $\tilde{\omega}_z$ contours and axial variation of y-z plane averaged contributions (i.e., the four terms on the right-hand side of Eq. (1)) to $\partial\tilde{\omega}_z/\partial t$. (a) t^*=7.35; (b) t^*=7.55; (c) t^*=7.85.

4. Conclusions

The following conclusions are drawn from the results presented:

1. By way of adequate spanwise and transverse perturbations, the present simulation of the spatially evolving turbulent supersonic/subsonic compressible mixing layer (M_c=0.51<critical M_c=0.6) successfully captures the various characteristic structures, particularly the well-organized chain-link-fence type structures, observed experimentally in the incompressible mixing layer (M_c=0). Such a computational study has received very limited attention in the past.
2. The presence of spanwise disturbances of the cross-stream velocity is essential to triggering the generation of streamwise vortices in an original 2-D compressible mixing layer (M_c<0.6) featured by large-scale spanwise vortical structure only.
3. wIt is found that during the spatial evolvement of the turbulent supersonic/subsonic mixing layers (M_c<0.6), both the streamwise and spanwise vorticity dynamics are dominated by the convection effect followed by the vortex stretching effect.

Acknowledgments

The research was supported by the National Science Council of the Republic of China under Contract NSC84-2212-E007-049.

References

Bernal, L. P., and Roshko, A., Streamwise Vortex Structure in Plane Mixing Layers, Journal of Fluid Mechanics, 170 (1986), 499-525.

Breidenthal, R., Structure in Turbulent Mixing Layers and Wakes Using a Chemical Reaction, Journal of Fluid Mechanics, 109 (1981), 1-24.

Brown, G. L., and Roshko, A., On density Effects and Large Structures in Turbulent Mixing Layers, Journal of Fluid Mechanics, 6 4 (1974), 775-816.

Chandrsuda, C., Mehta, R. D., Weir, A. D., and Bradshaw, P., Effect of Free-Stream Turbulence on Large Structure in Turbulent Mixing Layers, Journal of Fluid Mechanics, 85-4 (1978), 693-704.

Gathmann, R. J., Si-Ameur, M., and Mathey, F., Numerical Simulations of Three-Dimensional Natural Transition in the Compressibl e Confined Shear Layer, Physics of Fluids A, 5-11 (1993), 2946-2968.

Grinstein, F. F., Oran, E. S., and Hussain, F., Three-Dimensional Numerical Simulation of a Compressible, Spatially Evolving Mi xing Layer, AIAA Paper 88-0042, (1988).

Jimenez, J., A Spanwise Structure in the Plane Shear Layer, Journal of Fluid Mechanics, 132 (1983), 319-336.

Koochesfahani, M. M., Dimotakis, P. E., and Broadwell, J. E., A "Flip" Experiment in a Chemically Reacting Turbulent Mixing Layer, AIAA Journal, 23-8 (1985), 1191-1194.

Lasheras, J. C., Cho, J. S., and Maxworthy, T., On the Original and Evolution of Streamwise Vortical Structures in a Plane Free Shear Layer, Journal of Fluid Mechanics, 172 (1986), 231-258.

Leep, L. J., Dutton, J. C., and Burr, R. F., Three-Dimensional Simulations of Compressible Mixing Layers: Visualizations and Statistical Analysis, AIAA Journal, 31-11 (1993), 2039-2046.

Lele, S. K., Compressibility Effects on Turbulence, Annual Review of Fluid Mechanics, 26 (1994), 211-254.

Liou, T. M., Lien, W. Y., and Hwang, P. W., Compressibility Effects and Mixing Enhancement in Turbulent Free Shear Flows, AIAA Journal, 33-12 (1995), 2332-2338.

Liou, T. M., Lien, W. Y., and Hwang, P.W., Transition Characteristics of Flowfield in a Simulated Solid-Rocket Motor, Journal o f Propulsion and Power, 14-3 (1998), 282-289.

Liou, T. M., and Hwang, P.W., Numerical Visualization and Residence Time Determination of Turbulent Reacting Duct Flow with Mass Bleed and a Backstep on One Wall, Proceedings of the 27th International Symposium on Combustion (Boulder), 1998.

Liou, T. M., and Hwang, P.W., Visualization of Supersonic-Sudsonic Turbulent Free Shear Flows:Comparison Between 2D and 3D Computations, Proceeding of the 2nd Pacefic Symposium on Flow Visualization and Image Processing(Honolulu), 1999.

Nygaard, K. J., and Glezer, A., Core Instability of the Spanwise Vortices in a Plane Mixing Layer, Physics of Fluids A, 2-3 (19 90), 461-464.

Ragab, S., Sreedhar, M., and Mulholland, D., Large-Scale Structure in a Subsonic Mixing Layer, Physics of Fluids, 6-9 (1994), S7.

Sandham, N. D., and Reynolds, W. C., Three-Dimensional Simulations of Large Eddies in the Compressible Mixing Layer, Journal of Fluid Mechanics, 224 (1991), 133-158.

Samimy, M., and Elliott, G. S., Effects of Compressibility on the Characteristics of Free Shear Layers, AIAA Journal, 28-3 (199 0), 439-445.

Soetrisno, M., Greenough, J. A., Eberhardt, D. S., and Riley, J. J., Confined Compressible Mixing Layers: Part I. Three-Dimensi onal Instabilities, AIAA Paper 89-1810, (1989).

Winant, C. D., and Browand, F. K., Vortex Pairing: The Mechanism of Turbulent Mixing -Layer Growth at Moderate Reynolds Number, Journal of Fluid Mechanics, 63 (1974), 237-255.

Authors' Profiles

Tong-Miin Liou: He is a professor of Power Mechanical Engineering at National Tsing Hua University. He has advanced the technology of internal-combustion engines, solid-propellant rocket motors, ramjet engines and turbine blade internal cooling. He has authored 230 technical publications, and has won the 1985 SAE and 1991 CSME Best Paper Awards, 1995 CIE Engineering Prize, 1988-94 National Science Council Outstanding Research Awards and 1995-99 NSC Fellowship for Distinguished Professor. He was the first president of Chung Hua Polytechnic Institute. Liou is the President of the Combustion Institute of ROC and a Fellow of ASME. Ph.D. (1983), Princeton University.

Po-Wen Hwang: He is a Ph.D. candidate of Power Mechanical Engineering at National Tsing Hua University, Hsinchu, Taiwan, ROC.